1521-0103/358/2/230–238$25.00
THE JOURNAL OF PHARMACOLOGY AND EXPERIMENTAL THERAPEUTICS

http://dx.doi.org/10.1124/jpet.116.232876
J Pharmacol Exp Ther 358:230–238, August 2016

Chiral Plasma Pharmacokinetics and Urinary Excretion of Bupropion and Metabolites in Healthy Volunteers[S]

Andrea R. Masters, Brandon T. Gufford, Jessica Bo Li Lu, Ingrid F. Metzger, David R. Jones, and Zeruesenay Desta

Division of Clinical Pharmacology, Department of Medicine, Indiana University School of Medicine, Indianapolis, Indiana

Received March 23, 2016; accepted June 1, 2016

ABSTRACT

Bupropion, widely used as an antidepressant and smoking cessation aid, undergoes complex metabolism to yield numerous metabolites with unique disposition, effect, and drug–drug interactions (DDIs) in humans. The stereoselective plasma and urinary pharmacokinetics of bupropion and its metabolites were evaluated to understand their potential contributions to bupropion effects. Healthy human volunteers ($n = 15$) were administered a single oral dose of racemic bupropion (100 mg), which was followed by collection of plasma and urine samples and determination of bupropion and metabolite concentrations using novel liquid chromatography–tandem mass spectrometry assays. Time-dependent, elimination rate–limited, stereoselective pharmacokinetics were observed for all bupropion metabolites. Area under the plasma concentration-time curve from zero to infinity ratios were on average approximately 65, 6, 6, and 4 and C_{max} ratios were approximately 35, 6, 3, and 0.5 for (2*R*,3*R*)-/(2*S*,3*S*)-hydroxybupropion, *R*-/*S*-bupropion, (1*S*,2*R*)-/(1*R*,2*S*)-erythrohydrobupropion, and (1*R*,2*R*)-/(1*S*,2*S*)-threohydrobupropion, respectively. The *R*-/*S*-bupropion and (1*R*,2*R*)-/(1*S*,2*S*)-threohydrobupropion ratios are likely indicative of higher presystemic metabolism of *S*- versus *R*-bupropion by carbonyl reductases. Interestingly, the apparent renal clearance of (2*S*,3*S*)-hydroxybupropion was almost 10-fold higher than that of (2*R*,3*R*)-hydroxybupropion. The prediction of steady-state pharmacokinetics demonstrated differential stereospecific accumulation [partial area under the plasma concentration-time curve after the final simulated bupropion dose (300–312 hours) from 185 to 37,447 nM·h] and elimination [terminal half-life of approximately 7–46 hours] of bupropion metabolites, which may explain observed stereoselective differences in bupropion effect and DDI risk with CYP2D6 at steady state. Further elucidation of bupropion and metabolite disposition suggests that bupropion is not a reliable in vivo marker of CYP2B6 activity. In summary, to our knowledge, this is the first comprehensive report to provide novel insight into mechanisms underlying bupropion disposition by detailing the stereoselective pharmacokinetics of individual bupropion metabolites, which will enhance clinical understanding of bupropion's effects and DDIs with CYP2D6.

Introduction

Bupropion (BUP), a dual dopamine-norepinephrine uptake inhibitor (Ascher et al., 1995) and nicotine receptor antagonist (Fryer and Lukas, 1999), is widely used to manage depression and as a smoking cessation aid (Ascher et al., 1995; Hurt et al., 1997; Dwoskin et al., 2006; Dhillon et al., 2008). A combination of BUP and naltrexone was recently approved by the U.S. Food and Drug Administration for weight management (Yanovski and Yanovski, 2015), and BUP has been tested for multiple other indications (Dwoskin et al., 2006; Dhillon et al., 2008; Aubin et al., 2014). However, BUP use is associated with large interpatient variability in clinical response (Hurt et al., 1997; Jorenby et al., 1999; Dale et al., 2001; Thase et al., 2005). Some patients are at increased risk for adverse effects, such as dose-dependent seizures (Davidson, 1989), and there is a lack of biomarkers to identify at-risk patients. In addition, BUP causes clinically significant pharmacokinetic drug–drug interactions (DDIs) with CYP2D6 substrates (Kennedy et al., 2002; Kotlyar et al., 2005; Reese et al., 2008; Desmarais and Looper, 2009; Yee et al., 2014).

Understanding variable BUP effects and associated DDIs requires detailed knowledge of its metabolism and disposition. The first evidence linking BUP metabolism to effect was observed when BUP was shown to be more effective in mouse models of depression than in rat models of depression (Soroko

This research was supported by the National Institutes of Health National Institute of General Medical Sciences [Grants R01GM078501 and T32GM008425 (to B.T.G.)]. Bioanalyses were performed by the Clinical Pharmacology Analytical Core laboratory, a core laboratory of the Indiana University Melvin and Bren Simon Cancer Center supported by the National Institutes of Health National Cancer Institute [Grant P30CA082709].

A.R.M. and B.T.G. contributed equally to this work.

dx.doi.org/10.1124/jpet.116.232876.

[S] This article has supplemental material available at jpet.aspetjournals.org.

ABBREVIATIONS: AUC, area under the curve; $AUC_{0-\infty}$, area under the plasma concentration-time curve from zero to infinity; AUC_{0-last}, area under the curve from time zero to C_{last}; BUP, bupropion; CL/F, apparent oral clearance; CL_r, apparent renal clearance; DDI, drug–drug interaction; ERY, racemic erythrohydrobupropion; ERYHBUP, erythrohydrobupropion; ICRC, Indiana Clinical Research Center; LC, liquid chromatography; MS/MS, tandem mass spectrometry; OHBUP, 4-hydroxybupropion; *R*-BUP, (*R*)-bupropion; *RR*-OHBUP, (2*R*,3*R*)-hydroxybupropion; *RR*-THRHBUP, (1*R*,2*R*)-threohydrobupropion; *RS*-ERYHBUP, (1*R*,2*S*)-erythrohydrobupropion; *S*-BUP, (*S*)-bupropion; *SR*-ERYHBUP, (1*S*,2*R*)-erythrohydrobupropion; *SS*-OHBUP, (2*S*,3*S*)-hydroxybupropion; *SS*-THRHBUP, (1*S*,2*S*)-threohydrobupropion; $t_{1/2}$, terminal half-life; THR, racemic threohydrobupropion; THRHBUP, threohydrobupropion; T_{max}, time of maximal plasma concentration.

et al., 1977; Ferris et al., 1983). This species difference was later explained by the ability of mice to convert BUP to 4-hydroxybupropion (OHBUP) (active metabolite), whereas rats cleared BUP through alternate detoxification pathways (Suckow et al., 1986; Welch et al., 1987). In humans, BUP is cleared by extensive metabolism (Schroeder, 1983; Welch et al., 1987). Numerous BUP metabolites have been identified (Welch et al., 1987; Petsalo et al., 2007; Gufford et al., 2016), but OHBUP, threohydrobupropion (THRHBUP), and erythrohydrobupropion (ERYHBUP) are of primary interest to understand BUP's effect and DDIs. BUP is 4-hydroxylated by CYP2B6 to OHBUP (Faucette et al., 2000; Hesse et al., 2000; Benowitz et al., 2013), whereas the reduction of BUP by 11β-hydroxysteroid dehydrogenase 1 and other carbonyl reductases (Meyer et al., 2013; Connarn et al., 2015) forms two amino alcohol stereoisomers, THRHBUP and ERYHBUP. OHBUP, THRHBUP, and ERYHBUP exhibit pharmacological activity in preclinical models (Martin et al., 1990; Bondarev et al., 2003; Damaj et al., 2004, 2010) and may mediate BUP-induced seizures (Silverstone et al., 2008). In humans, these metabolites are believed to be responsible for BUP treatment outcomes (Daviss et al., 2006; Dwoskin et al., 2006; Lee et al., 2007; Zhu et al., 2012; Laib et al., 2014) and for clinically observed DDIs between BUP and CYP2D6 substrates (Reese et al., 2008; Parkinson et al., 2010; Yeung et al., 2011). The systemic exposure of OHBUP, THRHBUP, and ERYHBUP reaches up to 22-, 12-, and 2.7-fold higher, respectively, than BUP (Posner et al., 1985; Daviss et al., 2005; Benowitz et al., 2013). Exposure of these metabolites exhibits high intersubject variability (Zhu et al., 2012; Benowitz et al., 2013; Laib et al., 2014), but mechanisms underlying this variability are not fully understood.

BUP disposition is further complicated by being a chiral drug administered as a racemic mixture with limited understanding of the stereoselective metabolism. An additional chiral center is created when the hydroxyl intermediate spontaneously cyclizes to morpholinol and after reduction, potentially generating multiple diastereomers with unique disposition and effect profiles. Limited BUP and OHBUP data support striking stereoselective differences in their disposition (Suckow et al., 1997; Xu et al., 2007; Kharasch et al., 2008) and/or effect (Bondarev et al., 2003; Damaj et al., 2004; Carroll et al., 2014). This marked stereoselectivity is not fully explained by CYP2B6 alone (Coles and Kharasch, 2008) and other mechanisms appear important (Gufford et al., 2016). In contrast with OHBUP, data on the stereoselective disposition of THRHBUP and ERYHBUP are unavailable.

The purpose of this study was to determine stereospecific pharmacokinetics of BUP and its three major active metabolites and their respective glucuronides in healthy volunteers ($n = 15$) administered a single 100-mg oral dose of immediate-release racemic BUP. Recently developed novel chiral and achiral liquid chromatography (LC)–tandem mass spectrometry (MS/MS) methods facilitated the first separation and simultaneous quantification of enantiomers of BUP and diastereomers of its active (Masters et al., 2016) and downstream metabolites (Gufford et al., 2016). Information on stereoselective steady-state disposition of BUP and its metabolites is lacking. Thus, the single-dose pharmacokinetic data were modeled to predict steady-state stereoselective accumulation and exposure of BUP and its metabolites and inform the design of future studies.

Materials and Methods

Chemicals and Reagents

R-bupropion (*R*-BUP), *S*-bupropion (*S*-BUP), (2*R*,3*R*)-hydroxybupropion (*RR*-OHBUP), (2*S*, 3*S*)-hydroxybupropion (*SS*-OHBUP), racemic erythrohydrobupropion (ERY), racemic threohydrobupropion (THR), racemic erythrohydrobupropion (ERYHBUP) β-D-glucuronide, (1*R*,2*S*)-erythrohydrobupropion (*RS*-ERYHBUP) glucuronide, (1*R*,2*R*)-threohydrobupropion (*RR*-THRHBUP) β-D-glucuronide, and (1*S*,2*S*)-threohydrobupropion (*SS*-THRHBUP) β-D-glucuronide were purchased from Toronto Research Chemicals (Toronto, ON, Canada). Optically pure standards for racemic ERY and THR are not commercially available. Characterization of BUP enantiomers and glucuronides of its diastereomeric metabolites was described previously (Gufford et al., 2016). The internal standard, acetaminophen, and ammonium bicarbonate were purchased from Sigma Aldrich Chemical Co. (St. Louis, MO). High-performance LC–grade ammonium hydroxide, methanol, acetonitrile, sodium phosphate monobasic certified dehydrate, and ethyl acetate were purchased from Fisher Scientific (Fairlawn, NJ). Deionized water was purified using a Barnstead Nanopure Infinity ultrapure water system (Boston, MA). Plasma from human whole blood (tri-K EDTA, male, drug free, nonsmoker) for standard and quality control preparations was purchased from Biologic Specialty Corp. (Colmar, PA).

Clinical Study Protocol

Study Participants. A total of 15 nonsmoking, healthy female and male volunteers (aged 18–79 years), who were within 32% of their ideal body weight (Supplemental Table 1) were enrolled. Subjects were eligible to participate in the study if they agreed to refrain from taking any prescription medications, over-the-counter medications, hormonal agents, and herbal, dietary, and alternative supplements that may interact with the metabolism of BUP at least 2 weeks before the start of the study and until study completion. Approval to conduct the study was obtained, in advance, from the Institutional Review Board of the Indiana University School of Medicine and all participants signed an Institutional Review Board–approved informed consent form prior to enrollment. The trial is registered at ClinicalTrials.gov (identifier NCT02401256).

Study Design. On the day of the pharmacokinetic study, subjects arrived at the Indiana Clinical Research Center (ICRC; Indianapolis, IN) the morning after an overnight fast. Prior to BUP dosing, baseline blood (approximately 10 ml) and urine (approximately 50 ml) samples were collected. Subjects received a single 100-mg oral dose of immediate-release racemic BUP in a tablet form (National Drug Code 0781-1064-01, lot EM0855; Sandoz Inc., Princeton, NJ) by mouth on an empty stomach with approximately 250 ml water. A standard meal was served 3 hours after drug administration. While in the ICRC inpatient setting, blood (approximately 10 ml) was collected from the intravenous catheter at 0.5, 1, 1.5, 2, 2.5, 3, 4, 6, 8, 10, 12, 16, and 24 hours after BUP administration for pharmacokinetic evaluation. All urine voided during the 24-hour ICRC stay was collected in fractions of 0–12 and 12–24 hours. Urine from each of these intervals was collected in a different container. After the 24-hour blood sampling and urine collection, subjects were discharged home and given instructions and two urine containers to collect urine fractions for an additional day. One container was used for the 24- to 36-hour void and the second for the 36- to 48-hour void. Subjects returned to the ICRC outpatient on days 2 and 3 for collection of 48- and 72-hour blood samples (approximately 10 ml). Plasma was separated from whole blood by centrifugation at 3000 rpm for 20 minutes. Urine volumes voided at each interval after drug administration were recorded and two 10-ml aliquots were retained. Plasma and urine samples were immediately stored at −80°C until analysis.

Plasma Sample Analysis

R-BUP, *S*-BUP, *RR*-OHBUP, *SS*-OHBUP, *RR*-THRHBUP, *SS*-THRHBUP, *SR*-ERYHBUP, and *RS*-ERYHBUP were quantified from

plasma samples by high-performance LC-MS/MS (5500 QTRAP; AB Sciex, Framingham, MA) as previously reported by our group (Masters et al., 2016). Briefly, 50 μl plasma was used for the assay with acetaminophen added as the internal standard, followed by liquid–liquid extraction with ethyl acetate. Separation of all analytes was achieved using a Lux Cellulose-3 chiral column, 250 × 4.6 mm, 3 μm (Phenomenex, Torrance, CA). The limit of quantification was 0.3 ng/ml for *R*-BUP, *S*-BUP, *RR*-OHBUP, and *SS*-OHBUP. The low, medium, and high quality control concentrations were 1, 30, and 200 ng/ml. The limit of quantification was 0.15 ng/ml for *RR*-THRHBUP, *SS*-THRHBUP, *SR*-ERYHBUP, and *RS*-ERYHBUP. The low, medium, and high quality control concentrations were 0.5, 15, and 100 ng/ml. The intraday precision for all analytes ranged from 3.4% to 15.4% and the intraday accuracy ranged from 80.6% to 97.8%. The interday precision for all analytes ranged from 6.1% to 19.9% and the interday accuracy ranged from 88.5% to 99.9%.

Urine Sample Analysis

Urine concentrations of *S*- and *R*-BUP, *RR*- and *SS*-OHBUP, *SS*- and *RR*-THRHBUP, and *SR*- and *RS*-ERYHBUP were measured using the same LC-MS/MS method described above for plasma (Masters et al., 2016), with a minor modification (200 μl urine and 4 ml ethyl acetate was used). The limit of quantification for *R*-BUP, *S*-BUP, *RR*-OHBUP, and *SS*-OHBUP was 1 ng/ml. The limit of quantification for *RR*-THRHBUP, *SS*-THRHBUP, *SR*-ERYHBUP, and *RS*-ERYHBUP was 0.5 ng/ml.

Urine concentrations of glucuronides of *RR*- and *SS*-OHBUP, *SS*- and *RR*-THRHBUP, and *SR*- and *RS*-ERYHBUP were measured using an API 3200 triple quadrupole mass spectrometer (Applied Biosystems, Foster City, CA), coupled with a high-performance LC method recently described by our group (Gufford et al., 2016). Briefly, acetaminophen was added to the urine sample (50 μl) as the internal standard and precipitation was performed with water/methanol [50:50 (v/v)]. Chromatographic separation was achieved using a Luna C18 -2, 150 × 4.6 mm, 5 μm (Phenomenex). Standard curves were generated to directly quantify the glucuronide metabolites of THRHBUP and ERYHBUP using the available glucuronide standards with a limit of quantification of 0.1 ng/ml. *RR*- and *SS*-OHBUP glucuronides were quantified using the standard curves of *RR*- and *SS*-THRHBUP glucuronides, respectively, because analytical standards were not commercially available for diastereomers of OHBUP glucuronides. Attempts to obtain these standards commercially as well as analysis after deconjugation with β-glucuronidase proved unsuccessful. Ionization efficiency and other system parameters may yield the differing LC-MS/MS response between these structurally related metabolites. Thus, the reported nanomolar urinary excretion rates of *RR*- and *SS*-OHBUP glucuronides are more appropriately viewed as nanomolar equivalents relative to THRHBUP glucuronides with the same isomeric configuration.

Pharmacokinetic Analysis

Noncompartmental analysis of data was performed using Phoenix WinNonlin (version 6.4; Pharsight Corp., Cary, NC). Pharmacokinetic outcomes for analysis included the terminal half-life ($t_{1/2} = 0.693/k_{el}$), maximal plasma concentration (C_{max}), time of maximal plasma concentration (T_{max}), area under the plasma concentration-time curve from zero to infinity ($AUC_{0-\infty}$), volume of distribution calculated by clearance/k_{el}, and apparent oral clearance (CL/F), which was calculated as (CL/F) = dose/area under the curve. The terminal elimination-rate constant (λ_z) was estimated by linear regression of the terminal portion of the log-transformed concentration-time profile using at least three data points. The terminal half-life ($t_{1/2}$) was calculated as $\ln(2)/\lambda_z$. The maximum observed concentration (C_{max}), time to reach C_{max} (T_{max}), and last measured concentration (C_{last}) were recovered directly from the concentration-time profile. The area under the curve from time zero to C_{last} (AUC_{0-last}) was determined using the trapezoidal rule with linear-up/log-down interpolation. The $AUC_{0-\infty}$ was calculated as the sum of AUC_{0-last} and the ratio of C_{last} to λ_z. $AUC_{0-\infty}$ values reported for analytes where the extrapolation percentage was in excess of 30% are denoted accordingly. Steady-state concentration-time profiles were predicted from single-dose data using nonparametric superposition of individual subject data (n = 15) via Phoenix WinNonlin. The accumulation indices for BUP and metabolites were calculated as the absolute value of the inverse of $(1 - e^{-\lambda z \tau})$, where τ is equal to the dosing interval (τ = 12 hours for twice-daily BUP dosing). Steady-state pharmacokinetics outcomes were recovered using standard noncompartmental approaches as outlined above. Urinary excretion kinetics were analyzed both as absolute (nanogram) and molar (nanomolar) amounts (based on individual urine collection volumes) of each metabolite in relation to BUP using Phoenix WinNonlin. All urine concentrations were normalized using the individual urine volume for each collection interval. Apparent renal clearance (CL_r) was calculated as the body weight–normalized ratio of the cumulative amount excreted in the urine by 48 hours to the area under the plasma concentration-time curve during the same interval (in liters per hour per kg). Statistical data comparisons between the pharmacokinetic outcomes of the enantiomers were evaluated using a paired two-tailed t test on untransformed data (CL/F, area under the curve, $t_{1/2}$, C_{max}) or Wilcoxon signed-rank test (T_{max}) as appropriate. A P value < 0.05 was considered statistically significant. All statistical analyses were conducted using IBM SPSS software (version 23; IBM, Armonk, NY).

Results

Single-Dose Pharmacokinetics of BUP and Metabolites

The plasma concentration-time profiles of racemic and stereoisomers of BUP and metabolites in 15 healthy volunteers given a single 100-mg oral dose of BUP are shown in Fig. 1. The corresponding pharmacokinetic parameters and the stereospecific plasma concentration ratios over time are

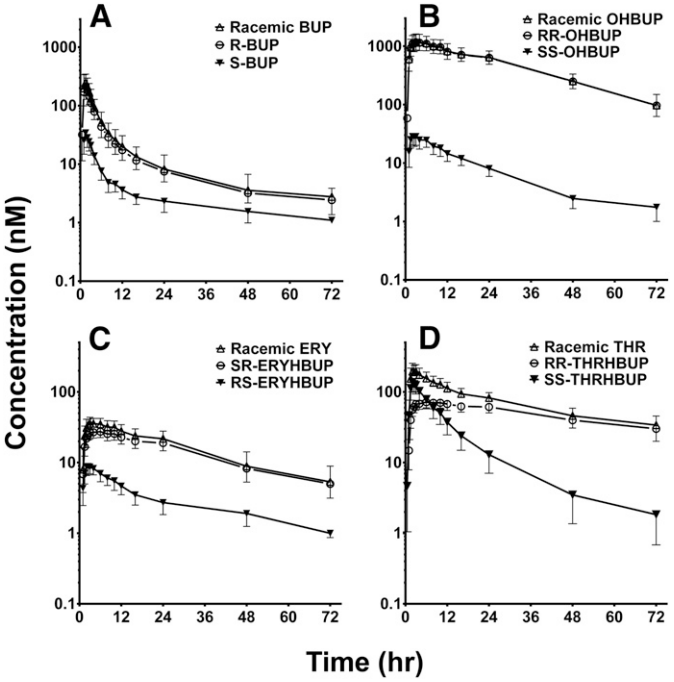

Fig. 1. Geometric mean concentration-time profiles of (A) racemic BUP, *R*-BUP, and *S*-BUP; (B) racemic OHBUP, *RR*-OHBUP, and *SS*-OHBUP; (C) racemic ERY, *SR*-ERYHBUP, and *RS*-ERYHBUP; and (D) THR, *RR*-THRHBUP, and *SS*-THRHBUP in 15 healthy volunteers after a single 100-mg oral dose of racemic BUP. Symbols and error bars denote observed geometric means and limits of the 95% confidence interval, respectively.

TABLE 1

Pharmacokinetic outcomes of racemic and enantiomers of BUP and metabolites in healthy volunteers (n = 15) administered a single 100-mg oral dose of BUP

T_{max} values are presented as the median (range). All other outcomes reported as the geometric mean (percent coefficient of variation) unless otherwise indicated. Dash indicates that no ratio was calculated.

Analyte	Pharmacokinetic Outcome						
	$t_{1/2}$	C_{max}	T_{max}	AUC_{0-last}	$AUC_{0-\infty}$	V_d/F	CL/F
	h	*nM*	*h*	*nM· h*		*l/kg*	*l/h*
Enantiomer							
R-BUP	11.6 (49)	288 (74)	1 (1–2.5)	1103 (61)	1,162 (58)	40.7 (78)	179 (58)
S-BUP	7.2 (103)	47.0 (74)	1.5 (1–3)	173 (74)	193 (72)	152 (83)	1,080 (72)
BUP (*R*-/*S*-)[a]	1.6 (1.1–2.4)	6.1 (5.3–7.1)	—	6.3 (5.5–7.3)	6.0 (5.2–7.0)	0.26 (0.2–0.36)	0.17 (0.14–0.19)
RR-OHBUP	19.3 (20)	1240 (55)	2.5 (1–10)	32,849 (46)	37,421 (49)		
SS-OHBUP	14.6 (36)	35.9 (74)	2.5 (1–6)	513 (56)	580 (55)		
OHBUP (*RR*-/*SS*-)[a]	1.3 (1.2–1.5)	34.7 (28.6–42.1))	—	64.0 (53.8–76.1)	64.5 (55.4–75.1)		
SR-ERYHBUP	24.2 (39)	30.5 (37)	3 (1–10)	942 (54)	1182 (60)		
RS-ERYHBUP	14.6 (61)	10.6 (52)	2 (1–4)	143 (74)	185 (71)		
ERY (*SR*-/*RS*-)[a]	1.7 (1.3–2.1)	2.9 (2.4–3.5)	—	6.6 (5.3–8.3)	6.4 (5.1–8.0)		
RR-THRHBUP	45.5 (40)	79.9 (34)	6 (1–12)	3326 (43)	5527 (61)[b]		
SS-THRHBUP	8.2 (48)	168 (67)	2 (1-4)	1393 (83)	1433 (84)		
THR (*RR*-/*SS*-)[a]	5.5 (4.2–7.3)	0.47 (0.38–0.60)	—	2.3 (1.6–3.3)	3.9 (2.6–5.7)		
Racemic							
BUP	10.8 (54)	335 (73)	1 (1–2.5)	1246 (65)	1334 (61)	65.7 (80)	312 (61)
OHBUP	19.2 (21)	1280 (56)	2.5 (1–10)	33,409 (46)	37,984 (49)		
ERY	21.6 (36)	40.0 (37)	2.5 (1–10)	1103 (53)	1330 (57)		
THR	30.8 (41)	235 (53)	2 (1–4)	4964 (41)	6632 (45)		

V_d, volume of distribution.
[a]These ratios are geometric mean ratios (90% confidence intervals).
[b]Extrapolation exceeded 30%.

illustrated in Table 1 and Fig. 2, respectively. Racemic BUP, OHBUP, and ERYHBUP have similar plasma concentration-time profiles compared with *R*-BUP, *RR*-OHBUP, and *SR*-ERYHBUP, respectively, whereas *S*-BUP, *SS*-OHBUP, and *RS*-ERYHBUP concentrations were much lower than the respective stereoisomer pair or racemic mixture (Fig. 1, A–C), illustrating marked stereoselective disposition. *RR*-OHBUP had a statistically significantly ($P < 0.001$) greater $AUC_{0-\infty}$, almost 65-fold higher, than SS-OHBUP and a 35-fold higher C_{max}. The $AUC_{0-\infty}$ of *RR*-OHBUP was over 32-fold greater than *R*-BUP, with a C_{max} about 4-fold greater than *R*-BUP. The mean $t_{1/2}$ was longer for *RR*-OHBUP (19.3 hours) compared with *SS*-OHBUP (14.6 hours) and *R*-BUP (11.6 hours). *SR*-ERYHBUP and *R*-BUP had similar $AUC_{0-\infty}$ values, as did *RS*-ERYHBUP, compared with *S*-BUP. *SR*-ERYHBUP had over 6-fold greater $AUC_{0-\infty}$ values than *RS*-ERYHBUP, a significantly ($P < 0.01$) higher $t_{1/2}$, and almost 3-fold higher C_{max}. *SR*-ERYHBUP had the second longest elimination $t_{1/2}$ of all of the analytes, at a mean $t_{1/2}$ of 24.2 hours. Plasma ratios of the respective stereoisomer pairs BUP, OHBUP, and ERYHBUP over time are displayed in Fig. 2, A–C, respectively. The observed ratios are much greater than 1, indicating marked stereoselective disposition. Although the *R*-/*S*-BUP ratios declined over time in a biphasic manner (sharp decline between 0.5 and 3 hours and then reversal up to 5.5 hours) (Fig. 2A), those of *RR*-/*SS*-OHBUP (Fig. 2B) and S*R*-/*RS*-ERYHBUP (Fig. 2C) increased over time.

Similar to the other analytes, the disposition of THRHBUP was stereoselective (Fig. 1D), but the pharmacokinetics of the two diastereomers show unique and interesting profiles compared with the other analytes. *RR*- and *SS*-THRHBUP show the most significant difference between the racemic and diastereomer profiles (Fig. 1D). Higher concentrations were observed for *SS*-THRHBUP compared with *RR*-THRHBUP up to 6 hours after BUP administration and showed the opposite thereafter. The plasma exposure of *RR*-THRHBUP was the second highest of all of the analytes and had the longest T_{max} (median approximately 6 hours), whereas the T_{max} of *SS*-THRHBUP was 2 hours. The *RR*-THRHBUP mean

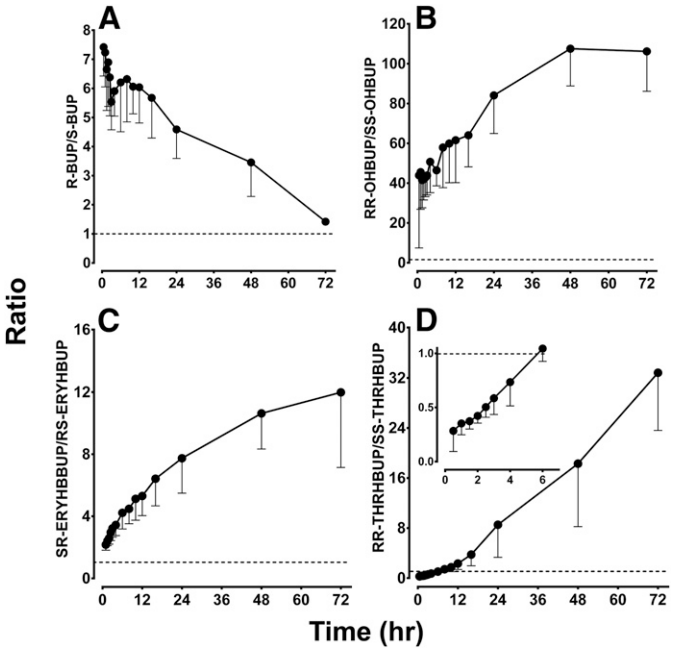

Fig. 2. Mean metabolic ratios of (A) *R*-BUP/S-BUP, (B) *RR*-OHBUP/*SS*-OHBUP, (C) *SR*-ERYHBUP/*RS*-ERYHBUP, and (D) *RR*-THRHBUP/*SS*-THRHBUP over time in 15 healthy volunteers after a single 100-mg oral dose of racemic BUP. The inset in (D) illustrates the switch in ratio directionality after 6 hours. Symbols and error bars denote observed mean ratios and lower limits of the 95% confidence interval, respectively.

AUC_{0-last} was approximately 2.4-fold higher than the AUC_{0-last} of *SS*-THRHBUP and approximately 3-fold greater than *S*-BUP. Although the AUC_{0-last} was greater for *RR*-THRHBUP than *SS*-THRHBUP, a significantly ($P < 0.001$) higher C_{max} (168 nM) was noted for *SS*-THRHBUP compared with *RR*-THRHBUP (79.9 nM). In fact, the early concentration versus time profile of *SS*-THRHBUP reflects the expected behavior if this metabolite were to be directly administered orally, suggesting that it might be efficiently formed in the gut wall.

The individual relative plasma exposure ($AUC_{0-\infty}$) of racemic and stereoisomers of BUP and metabolites is shown in Table 1. On the basis of racemic plasma exposure, OHBUP, THRHBUP, and ERYHBUP were on average 37-, 5.6-, and 1.2-fold higher than that of BUP (Fig. 2; Table 1). *RR*-OHBUP, *RR*-THRHBUP, and *SR*-ERYHBUP are the foremost contributors to the observed exposure of racemic OHBUP, THRHBUP, and ERYHBUP, respectively (Figs. 2 and 4B; Table 1). Further evidence of elimination rate–limited kinetics is apparent from the plasma concentration-time curves. Excluding *SS*-OHBUP (Fig. 3E), all analytes have significantly slower elimination rates than the respective parent substrate (Fig. 3, A, B, D, G, and H; Table 1). *SS*-OHBUP has a similar elimination rate to *S*-BUP ($t_{1/2}$ = 8 versus 7 hours) but a much higher AUC, potentially confounding its use as an in vivo probe of CYP2B6 activity (Fig. 3B; Table 1). The ratios of *RR*-OHBUP/*R*-BUP were much higher and parallel to those *SS*-OHBUP/*S*-BUP (Fig. 3C), indicating proportional formation or elimination relative to their respective enantiomers of BUP. The ratios of *SR*-ERYHBUP/*R*-BUP overlapped with those of *RS*-ERYHBUP/*S*-BUP at least in the first 12 hours after BUP administration (Fig. 3F). It appears that *S*-BUP is more efficiently converted to *RS*-ERYHBUP than *R*-BUP is to *SR*-ERYHBUP. The ratios of *RR*-THRHBUP/*R*-BUP are much lower than the ratios of *SS*-THRHBUP/*S*-BUP up to 12 hours after BUP administration (Fig. 3I).

Enantioselective Urinary Excretion of BUP and Metabolites

Approximately 12% of the administered BUP dose was recovered in the urine as parent and metabolites by 48 hours. In concurrence with a previous report (Benowitz et al., 2013), only 0.3% of the administered BUP dose was recovered in the urine as unchanged drug, with nearly 6-fold greater mean urinary recovery of *R*- versus *S*-BUP (Table 2). Urinary excretion analysis revealed stereoselective elimination of BUP, primary metabolites, and glucuronide conjugates (Table 2). *RR*-THRHBUP, the predominant BUP primary metabolite detected in urine, and *SS*-THRHBUP together accounted for nearly 30% of all BUP species measured in the urine (Table 2). The most prevalent urinary BUP metabolites, *RR*-THRHBUP and the glucuronide conjugate of *RR*-OHBUP, are excreted in similar amounts, suggesting that metabolism via carbonyl reductases and glucuronidation are among the most important contributors to overall BUP disposition. Urinary excretion reveals approximately 1.8-fold greater recovery of *RR*-THRHBUP versus *SS*-THRHBUP at 48 hours, in concurrence with the observed 2.3-fold greater plasma exposure (AUC_{0-last}) of *RR*-THRHBUP. The most abundant BUP species detected in plasma, *RR*-OHBUP, coincides with the most prevalent glucuronide conjugate detected in urine, *RR*-OHBUP glucuronide. The *SS*-OHBUP CL_r was, on average, nearly 10-fold greater than that of *RR*-OHBUP (Table 2). The CL_r values of enantiomers of BUP and diastereomers of ERYHBUP and THRHBUP were similar within each enantiomer pair (Table 2).

Prediction of Steady-State BUP and Metabolite Exposure

Steady-state concentration-time predictions demonstrate marked enantioselective accumulation of BUP metabolites. Accumulation indexes ranged from 1.6 to 6.0, with *RR*-THRHBUP and *SS*-THRHBUP representing the two extremes (Fig. 4; Table 3). Prediction of steady-state exposure from single-dose data suggests that enantioselective accumulation of *RR*-THRHBUP leads to plasma exposure exceeding that of all other metabolites, with the exception of *RR*-OHBUP (Fig. 4; Table 3). Predicted steady-state exposure varied greater than 200-fold across the analytes evaluated. In contrast with single-dose observations, *RR*-THRHBUP maximal steady-state concentrations are predicted to exceed those

TABLE 2

Forty-eight–hour BUP and metabolite urinary excretion

Values denote the geometric mean (90% confidence intervals) for 15 subjects.

Analyte	48-h Recovery	Percentage of BUP Dose	CL_r[b]
	nmol		*l/h*
Enantiomer			
R-BUP	1106 (873–1401)	0.27 (0.21–0.34)	1.00 (0.71–1.41)
S-BUP	197 (164–238)	0.05 (0.04–0.06)	1.07 (0.79–1.45)
RR-OHBUP	4180 (3167–5517)	1.00 (0.76–1.32)	0.14 (0.10–0.18)
SS-OHBUP	655 (508–845)	0.16 (0.12–0.20)	1.28 (1.03–1.59)
RR-THRHBUP	10,361 (8433–12,729)	2.48 (2.02–3.05)	3.88 (3.02–4.97)
SS-THRHBUP	4391 (2887–6679)	1.05 (0.69–1.60)	3.18 (2.01–5.03)
SR-ERYHBUP	2120 (1710–2628)	0.51 (0.41–0.63)	2.51 (1.95–3.24)
RS-ERYHBUP	374 (282–497)	0.09 (0.07–0.12)	2.36 (1.64–3.40)
Glucuronide			
RR-OHBUP Gluc[a]	15,751 (12,598–19,693)	3.78 (3.02–4.72)	—
SS-OHBUP Gluc[a]	5301 (4228–6646)	1.27 (1.01–1.59)	—
RR-THRHBUP Gluc	3782 (2879–4969)	0.91 (0.69–1.19)	—
SS-THRHBUP Gluc	969 (827–1135)	0.23 (0.20–0.27)	—
SR-ERYHBUP Gluc	1878 (1569–2247)	0.45 (0.38–0.54)	—
RS-ERYHBUP Gluc	382 (302–482)	0.09 (0.07–0.12)	—

[a] *RR*-OHBUP and *SS*-OHBUP glucuronides represent nanomolar equivalents relative to THRHBUP glucuronides with the same isomeric configuration.

[b] CL_r is calculated as the ratio of the cumulative amount excreted in the urine by 48 hours to the area under the plasma concentration-time curve during the same interval.

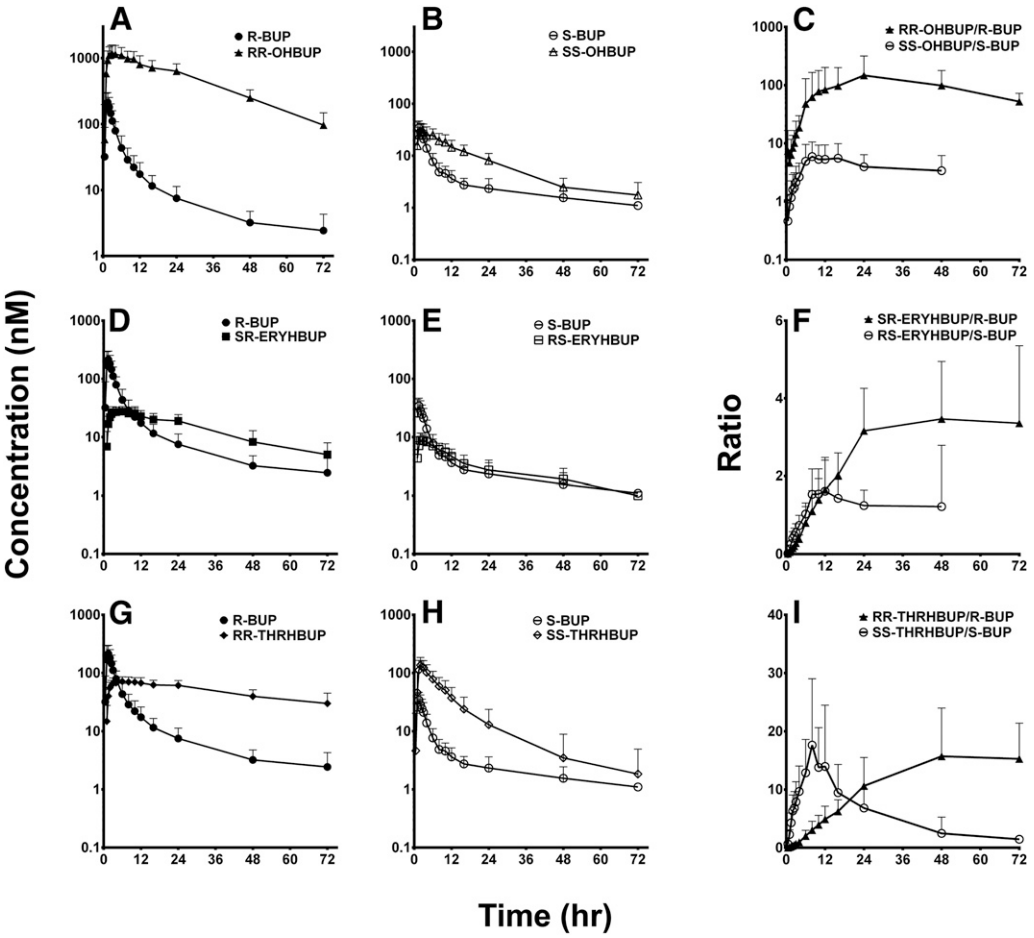

Fig. 3. Geometric mean concentration-time profiles and ratios of BUP metabolites and predicted substrates (denoted as predicted substrate → predicted metabolite) based on proposed metabolic pathways: (A) *R*-BUP → *RR*-OHBUP , (B) *S*-BUP → *SS*-OHBUP, and (C) ratios of *RR*-OHBUP/*R*-BUP and SS-OHBUP/S-BUP, (D) *R*-BUP → *SR*-ERYHBUP, (E) *S*-BUP → (1*R*,2*S*)- OHBUP, (F) *SR*-ERYHBUP/*R*-BUP and *RS*-ERYHBUP/*S*-BUP, (G) *R*-BUP → (1*R*,*2R*)-OHBUP, (H) *S*-BUP → (1*S*,2*S*)-OHBUP, and (I) *RR*-THRHBUP/*R*-BUP and *SS*-THRHBUP/*S*-BUP. The log-transformed ratio over time is depicted in (C, F, and I) for graphical clarity. Symbols and error bars denote observed geometric means and limits of the 95% confidence interval, respectively.

of both *SS*-THRHBUP and *R*-BUP. Approximately 5 days after termination of BUP administration, *RR*-THRHBUP plasma concentrations are predicted to exceed those of all other metabolites as a result of relatively slow, stereospecific elimination (Fig. 4B).

Discussion

BUP, administered orally as a racemic mixture, is stereoselectively metabolized in humans, yielding numerous primary and secondary metabolites. To our knowledge, this is the first comprehensive stereoselective analysis of BUP and its individual active metabolites in plasma and urine from healthy volunteers administered a single 100-mg oral dose of racemic BUP (equimolar *R*- and *S*-BUP). Individual THRHBUP and ERYHBUP diastereomers were separated and quantified to, for the first time, reveal marked stereospecific disposition in both plasma and urine. Stereospecific differential accumulation and exposure at steady state as well as a differential off rate after discontinuation of BUP therapy were predicted using single-dose pharmacokinetic data because stereoselective steady-state BUP kinetics have not been reported previously. These data, coupled with our recent in vitro report (Gufford et al., 2016), demonstrate that stereospecific BUP metabolism leads to unique pharmacokinetic behavior in vivo with potential therapeutic and toxic ramifications.

Detailed analysis of the plasma concentration (*R*-/*S*-BUP) ratios over time uncovered unique disposition characteristics. Ratios are higher at earlier time points and decline in a biphasic manner, indicative of differential gut and liver metabolism. Similarly, C_{max} and $AUC_{0-\infty}$ ratios of *R*-/*S*-BUP (approximately 6-fold), along with a time-dependent decline in the plasma concentration ratios, support that stereoselectivity is attributable to differences in *S*- and *R*-BUP apparent oral bioavailability. Our data suggest that *S*-BUP is a high-clearance enantiomer that preferentially undergoes presystemic reduction in the gut and liver primarily to *SS*-THRHBUP but also to *RS*-ERYHBUP, leading to lower oral bioavailability than *R*-BUP. Considering *S*-BUP as a prodrug that requires conversion by CYP2B6 to the pharmacologically active metabolite, *SS*-OHBUP (Carroll et al., 2014), genetic and nongenetic mechanisms affecting presystemic metabolism of *S*-BUP may have important clinical consequences.

Detailed understanding of the disposition of THRHBUP and ERYHBUP is important because of their potential

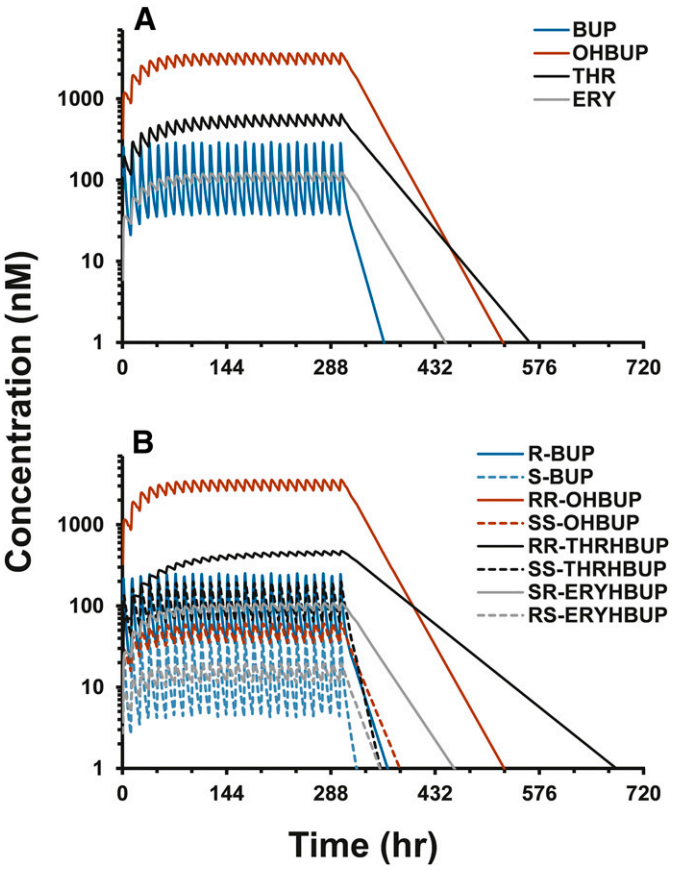

Fig. 4. Predicted steady-state geometric mean concentration-time profiles of (A) racemic BUP (blue), OHBUP (red), THR (black), and ERY (gray) and (B) individual enantiomers *R*-BUP (solid blue), *S*-BUP (dashed blue), *RR*-OHBUP (solid red), *SS*-OHBUP (dashed red), *RR*-THRHBUP (solid black), *SS*-THRHBUP (dashed black), *SR*-ERYHBUP (solid gray), and *RS*-ERYHBUP (dashed gray) after twice-daily oral BUP (100 mg) administration for 13 days, after which terminal elimination is depicted to 30 days.

TABLE 3

Predicted pharmacokinetic parameters of racemic and enantiomers of BUP and metabolites in healthy volunteers (n = 15) administered BUP (100 mg) to steady state

Values denote the geometric mean (90% confidence interval) or the percent coefficient of variation predicted using single-dose pharmacokinetic outcomes obtained from 15 subjects.

Analyte	Accumulation Index	C_{max}	AUC_{τ}
		nM	*nM· h*
Enantiomer			
R-BUP	2.0 (1.8–2.4)	324.4 (71)	1158 (58)
S-BUP	1.7 (1.4–2.0)	53.2 (72)	191 (72)
RR-OHBUP	2.9 (2.7–3.1)	3654.7 (50)	37,447 (49)
SS-OHBUP	2.3 (2.1–2.6)	68.5 (61)	577 (55)
RR-THRHBUP	6.0 (5.1–7.1)	490.4 (57)	5399 (57)
SS-THRHBUP	1.6 (1.4–1.8)	231.7 (75)	1433 (84)
SR-ERYHBUP	3.5 (3.0–4.0)	110.9 (57)	1182 (60)
RS-ERYHBUP	2.4 (2.0–2.9)	21.4 (63)	185 (71)
Racemic			
BUP	1.9 (1.7–2.2)	375.4 (71)	1331 (62)
OHBUP	2.9 (2.7–3.1)	3718.8 (50)	37,993 (49)
THR	4.3 (3.7–5.0)	682.8 (45)	6539 (44)
ERY	3.2 (2.8–3.6)	128.8 (54)	1330 (57)

AUC_{τ}, partial area under the plasma concentration-time curve after the final simulated bupropion dose (300–312 hours).

pharmacological activity, higher inhibitory potency (lower K_i) toward CYP2D6 (Reese et al., 2008), and relative abundance compared with the parent (Benowitz et al., 2013). Here, for the first time, we isolate diastereomers of THRHBUP and ERYHBUP, quantify them in human plasma and urine samples, and demonstrate their marked stereoselective disposition. Stereoselective THRHBUP disposition is demonstrated in Figs. 2D and 3D and Table 1, with unique pharmacokinetic characteristics as revealed by time-dependent changes in the plasma concentration ratios of *RR*-THRHBUP/*SS*-THRHBUP. Specifically, the C_{max} ratio was lower than 1 (the line of unity). Similarly, the plasma concentration ratios were substantially lower than 1 initially and then progressively above the line of unity from 6 hours up to 72 hours. These data indicate that the initial rate of formation for *SS*-THRHBUP is faster than the rate of *RR*-THRHBUP formation. Although the mechanism remains unknown, *SS*-THRHBUP is subsequently eliminated more rapidly than *RR*-THRHBUP. Considering that the proximate substrates of *RR*-THRHBUP and *SS*-THRHBUP identified in vitro are *R*- and *S*-BUP, respectively (Gufford et al., 2016; Masters et al., 2016), our data suggest that the metabolic conversion of *S*-BUP to form *SS*-THRHBUP is occurring at a faster rate than *RR*-THRHBUP is formed from *R*-BUP. A plausible explanation is that *S*-BUP more efficiently undergoes presystemic intestinal and hepatic metabolism via carbonyl reductases than *R*-BUP, leading to early appearance of *SS*-THRHBUP, with higher C_{max}, than *RR*-THRHBUP. The rapid biphasic decline in the ratio of *R*-BUP/*S*-BUP (Fig. 2A) within the first 6 hours corresponds well with the suggestion that *S*-BUP is metabolized presystemically in the intestine and the liver by carbonyl reductases at a much higher rate than *R*-BUP (Fig. 3I).

BUP 4-hydroxylation is exclusively catalyzed by CYP2B6 in vitro (Faucette et al., 2000; Hesse et al., 2000) and in vivo (Benowitz et al., 2013) to form the intermediate hydroxyl metabolite that spontaneously cyclizes to morpholinol, creating a second chiral center. Although four stereoisomers are expected, only two *trans*-diastereomers, *SS*- and *RR*-OHBUP, were detected in plasma and when synthesized de novo (Suckow et al., 1997; Carroll et al., 2010, 2014). These data are consistent with the suggestion that steric hindrance reduces cyclization to the *cis*-diastereomers, (2*R*,3*S*)- and (2*S*,3*R*)-OHBUP, and favors the thermodynamically more stable *trans*-isomers (Carroll et al., 2010). Our data provide evidence that mechanisms other than CYP2B6 appear to be responsible for the magnitude of OHBUP stereoselectivity. The in vitro rates of *S*-BUP hydroxylation in expressed CYP2B6 and human liver microsomes were only 3- and 1.5-fold higher, respectively, than *R*-BUP (Coles and Kharasch, 2008). Extensive presystemic *S*-BUP metabolism may cause shunting to parallel, non-CYP2B6 pathways and reduction of *S*-BUP bioavailability and availability for CYP2B6-mediated metabolism. This suggestion is supported by Figs. 1D and 2D displaying unique pharmacokinetics of the reductive metabolite generated from *S*-BUP. In addition, our data suggest that renal elimination of the two diastereomers is stereoselective because the renal clearance of *SS*-OHBUP was approximately 10-fold higher than that of *RR*-OHBUP (Table 2), although the mechanistic basis for this observation remains to be established. Although only racemic mixtures were previously studied in humans, OHBUP plasma exposure varies widely among patients, due in part to CYP2B6 genetic variation

(Benowitz et al., 2013), and this variability is associated with BUP treatment outcomes in both depression (Laib et al., 2014) and smoking cessation (Zhu et al., 2012).

Our data also have direct implications for the use of BUP 4-hydroxylation to OHBUP as an in vivo marker of CYP2B6 activity. This reaction has frequently been used to assess the effect of genetic and nongenetic factors influencing CYP2B6 activity in vitro and in vivo. However, the significant contribution of non-cytochrome P450–mediated pathways, the involvement of cytochrome P450 enzymes other than CYP2B6 in overall BUP metabolism, the elimination rate–limited kinetics of OHBUP, and the complex pharmacokinetics of BUP and its metabolites may limit the utility of racemic BUP as a quantitative in vivo probe of CYP2B6 activity (Palovaara et al., 2003; Turpeinen et al., 2005; Loboz et al., 2006; Kharasch et al., 2008; Ilic et al., 2013). This assertion is particularly important in assessment of DDIs mediated via induction (Xu et al., 2007) and functional consequences of genetic variants (Kirchheiner et al., 2003). The metabolism of *S*-BUP to *SS*-OHBUP has been suggested to improve BUP utility as an in vivo CYP2B6 probe (Kharasch et al., 2008) but limitations still exist. Several factors identified in our study confound the use of stereospecific BUP metabolism as an in vivo probe of CYP2B6 activity, including the enantioselective elimination rate–limited kinetics of BUP metabolites, the potentially important contribution of stereoselective gut and hepatic presystemic metabolism of *S*-BUP, and the observed stereospecific renal elimination of diastereomers of OHBUP. Taken together, analysis of the enantioselective metabolism and urinary elimination of BUP provides additional data to suggest that BUP may not be a reliable marker of CYP2B6 activity in vivo.

Prediction of steady-state metabolite exposure suggests stereoselective accumulation of pharmacologically active metabolites, which may contribute to observed interindividual differences in BUP therapeutic effects, toxicity, and DDIs. Clinically observed interactions of BUP with CYP2D6 substrates are poorly predicted from in vitro inhibition data (Kennedy et al., 2002; Kotlyar et al., 2005; Reese et al., 2008; Desmarais and Looper, 2009; Yee et al., 2014). Consideration of differential stereoselective pharmacokinetics coupled with stereoselective inhibition potency may help to explain these apparent in vitro–in vivo disconnects. However, comprehensive understanding of the formation and elimination clearance rates and enzymatic pathways contributing to metabolite disposition would be required to accurately predict in vivo behavior and relative contribution to DDIs (Lutz et al., 2010; Lutz and Isoherranen, 2012). The prolonged systemic exposure of *RR*-THRHBUP after discontinuation of BUP administration (Fig. 4B) may explain the observed persistence of BUP DDIs with CYP2D6 substrates long after the expected elimination of parent BUP from the systemic circulation. Knowledge of BUP stereoselective inhibition kinetics may improve translation of in vitro findings to clinical effects but remains unexplored.

In summary, to our knowledge, this is the first comprehensive stereoselective analysis of BUP and its individual active metabolites in human plasma and urine. We recognize several limitations in the reported study. First, the lack of available standards to directly quantify the glucuronides of OHBUP precludes absolute determination of the amount eliminated in the urine. Synthesis or isolation of these two compounds could enhance the quantitative analysis of future BUP pharmacokinetic studies. Second, sampling times were originally designed to capture BUP and OHBUP kinetics as a secondary probe of CYP2B6 activity. As such, the sampling duration was inadequate for complete capture of plasma pharmacokinetics and urinary elimination of all individual metabolites. However, it was impossible to predict optimal sampling times for these analytes in the absence of relevant in vivo pharmacokinetic data, presented for the first time in this work. These data will serve as the basis for appropriate design of future studies to further explore BUP metabolite kinetics. Nevertheless, our data provide novel insight into tissue- and enzyme-dependent mechanisms of stereoselective metabolism and offer a potential explanation of the drastically lower *S*-BUP and *SS*-OHBUP exposure compared with *R*-BUP and *RR*-OHBUP. Because there are no steady-state data regarding stereoselective disposition of BUP, our prediction of stereospecific differential exposure and accumulation should inform the design of future studies to link observed enantioselective differences in BUP exposure to effects and DDI risk at steady state.

Authorship Contributions

Participated in research design: Masters, Gufford, Lu, Metzger, Desta.

Conducted experiments: Masters, Lu, Metzger.

Contributed new reagents or analytic tools: Masters, Lu, Jones, Desta.

Performed data analysis: Masters, Gufford, Jones, Desta.

Wrote or contributed to the writing of the manuscript: Masters, Gufford, Jones, Desta.

References

Ascher JA, Cole JO, Colin JN, Feighner JP, Ferris RM, Fibiger HC, Golden RN, Martin P, Potter WZ, and Richelson E, et al. (1995) Bupropion: a review of its mechanism of antidepressant activity. *J Clin Psychiatry* **56**:395–401.

Aubin HJ, Luquiens A, and Berlin I (2014) Pharmacotherapy for smoking cessation: pharmacological principles and clinical practice. *Br J Clin Pharmacol* **77**:324–336.

Benowitz NL, Zhu AZ, Tyndale RF, Dempsey D, and Jacob P, 3rd (2013) Influence of CYP2B6 genetic variants on plasma and urine concentrations of bupropion and metabolites at steady state. *Pharmacogenet Genomics* **23**:135–141.

Bondarev ML, Bondareva TS, Young R, and Glennon RA (2003) Behavioral and biochemical investigations of bupropion metabolites. *Eur J Pharmacol* **474**:85–93.

Carroll FI, Blough BE, Mascarella SW, Navarro HA, Eaton JB, Lukas RJ, and Damaj MI (2010) Synthesis and biological evaluation of bupropion analogues as potential pharmacotherapies for smoking cessation. *J Med Chem* **53**:2204–2214.

Carroll FI, Blough BE, Mascarella SW, Navarro HA, Lukas RJ, and Damaj MI (2014) Bupropion and bupropion analogs as treatments for CNS disorders. *Adv Pharmacol* **69**:177–216.

Coles R and Kharasch ED (2008) Stereoselective metabolism of bupropion by cytochrome P4502B6 (CYP2B6) and human liver microsomes. *Pharm Res* **25**: 1405–1411.

Connarn JN, Zhang X, Babiskin A, and Sun D (2015) Metabolism of bupropion by carbonyl reductases in liver and intestine. *Drug Metab Dispos* **43**:1019–1027.

Dale LC, Glover ED, Sachs DP, Schroeder DR, Offord KP, Croghan IT, and Hurt RD (2001) Bupropion for smoking cessation : predictors of successful outcome. *Chest* **119**:1357–1364.

Damaj MI, Carroll FI, Eaton JB, Navarro HA, Blough BE, Mirza S, Lukas RJ, and Martin BR (2004) Enantioselective effects of hydroxy metabolites of bupropion on behavior and on function of monoamine transporters and nicotinic receptors. *Mol Pharmacol* **66**:675–682.

Damaj MI, Grabus SD, Navarro HA, Vann RE, Warner JA, King LS, Wiley JL, Blough BE, Lukas RJ, and Carroll FI (2010) Effects of hydroxymetabolites of bupropion on nicotine dependence behavior in mice. *J Pharmacol Exp Ther* **334**: 1087–1095.

Davidson J (1989) Seizures and bupropion: a review. *J Clin Psychiatry* **50**:256–261.

Daviss WB, Perel JM, Brent DA, Axelson DA, Rudolph GR, Gilchrist R, Nuss S, and Birmaher B (2006) Acute antidepressant response and plasma levels of bupropion and metabolites in a pediatric-aged sample: an exploratory study. *Ther Drug Monit* **28**:190–198.

Daviss WB, Perel JM, Rudolph GR, Axelson DA, Gilchrist R, Nuss S, Birmaher B, and Brent DA (2005) Steady-state pharmacokinetics of bupropion SR in juvenile patients. *J Am Acad Child Adolesc Psychiatry* **44**:349–357.

Desmarais JE and Looper KJ (2009) Interactions between tamoxifen and antidepressants via cytochrome P450 2D6. *J Clin Psychiatry* **70**:1688–1697.

Dhillon S, Yang LP, and Curran MP (2008) Bupropion: a review of its use in the management of major depressive disorder. *Drugs* **68**:653–689.

Dwoskin LP, Rauhut AS, King-Pospisil KA, and Bardo MT (2006) Review of the pharmacology and clinical profile of bupropion, an antidepressant and tobacco use cessation agent. *CNS Drug Rev* **12**:178–207.

Faucette SR, Hawke RL, Lecluyse EL, Shord SS, Yan B, Laethem RM, and Lindley CM (2000) Validation of bupropion hydroxylation as a selective marker of human cytochrome P450 2B6 catalytic activity. *Drug Metab Dispos* **28**:1222–1230.

Ferris RM, Cooper BR, and Maxwell RA (1983) Studies of bupropion's mechanism of antidepressant activity. *J Clin Psychiatry* **44**:74–78.

Fryer JD and Lukas RJ (1999) Noncompetitive functional inhibition at diverse, human nicotinic acetylcholine receptor subtypes by bupropion, phencyclidine, and ibogaine. *J Pharmacol Exp Ther* **288**:88–92.

Gufford BT, Lu JB, Metzger IF, Jones DR, and Desta Z (2016) Stereoselective glucuronidation of bupropion metabolites in vitro and in vivo. *Drug Metab Dispos* **44**:544–553.

Hesse LM, Venkatakrishnan K, Court MH, von Moltke LL, Duan SX, Shader RI, and Greenblatt DJ (2000) CYP2B6 mediates the in vitro hydroxylation of bupropion: potential drug interactions with other antidepressants. *Drug Metab Dispos* **28**:1176–1183.

Hurt RD, Sachs DP, Glover ED, Offord KP, Johnston JA, Dale LC, Khayrallah MA, Schroeder DR, Glover PN, and Sullivan CR, et al. (1997) A comparison of sustained-release bupropion and placebo for smoking cessation. *N Engl J Med* **337**: 1195–1202.

Ilic K, Hawke RL, Thirumaran RK, Schuetz EG, Hull JH, Kashuba AD, Stewart PW, Lindley CM, and Chen ML (2013) The influence of sex, ethnicity, and CYP2B6 genotype on bupropion metabolism as an index of hepatic CYP2B6 activity in humans. *Drug Metab Dispos* **41**:575–581.

Jorenby DE, Leischow SJ, Nides MA, Rennard SI, Johnston JA, Hughes AR, Smith SS, Muramoto ML, Daughton DM, and Doan K, et al. (1999) A controlled trial of sustained-release bupropion, a nicotine patch, or both for smoking cessation. *N Engl J Med* **340**:685–691.

Kennedy SH, McCann SM, Masellis M, McIntyre RS, Raskin J, McKay G, and Baker GB (2002) Combining bupropion SR with venlafaxine, paroxetine, or fluoxetine: a preliminary report on pharmacokinetic, therapeutic, and sexual dysfunction effects. *J Clin Psychiatry* **63**:181–186.

Kharasch ED, Mitchell D, and Coles R (2008) Stereoselective bupropion hydroxylation as an in vivo phenotypic probe for cytochrome P4502B6 (CYP2B6) activity. *J Clin Pharmacol* **48**:464–474.

Kirchheiner J, Klein C, Meineke I, Sasse J, Zanger UM, Mürdter TE, Roots I, and Brockmöller J (2003) Bupropion and 4-OH-bupropion pharmacokinetics in relation to genetic polymorphisms in CYP2B6. *Pharmacogenetics* **13**:619–626.

Kotlyar M, Brauer LH, Tracy TS, Hatsukami DK, Harris J, Bronars CA, and Adson DE (2005) Inhibition of CYP2D6 activity by bupropion. *J Clin Psychopharmacol* **25**: 226–229.

Laib AK, Brünen S, Pfeifer P, Vincent P, and Hiemke C (2014) Serum concentrations of hydroxybupropion for dose optimization of depressed patients treated with bupropion. *Ther Drug Monit* **36**:473–479.

Lee AM, Jepson C, Hoffmann E, Epstein L, Hawk LW, Lerman C, and Tyndale RF (2007) CYP2B6 genotype alters abstinence rates in a bupropion smoking cessation trial. *Biol Psychiatry* **62**:635–641.

Loboz KK, Gross AS, Williams KM, Liauw WS, Day RO, Blievernicht JK, Zanger UM, and McLachlan AJ (2006) Cytochrome P450 2B6 activity as measured by bupropion hydroxylation: effect of induction by rifampin and ethnicity. *Clin Pharmacol Ther* **80**:75–84.

Lutz JD, Fujioka Y, and Isoherranen N (2010) Rationalization and prediction of in vivo metabolite exposures: the role of metabolite kinetics, clearance predictions and in vitro parameters. *Expert Opin Drug Metab Toxicol* **6**:1095–1109.

Lutz JD and Isoherranen N (2012) In vitro-to-in vivo predictions of drug-drug interactions involving multiple reversible inhibitors. *Expert Opin Drug Metab Toxicol* **8**:449–466.

Martin P, Massol J, Colin JN, Lacomblez L, and Puech AJ (1990) Antidepressant profile of bupropion and three metabolites in mice. *Pharmacopsychiatry* **23**:187–194.

Masters AR, McCoy M, Jones DR, and Desta Z (2016) Stereoselective method to quantify bupropion and its three major metabolites, hydroxybupropion, erythro-dihydrobupropion, and threo-dihydrobupropion using HPLC-MS/MS. *J Chromatogr B Analyt Technol Biomed Life Sci* **1015–1016**:201–208.

Meyer A, Vuorinen A, Zielinska AE, Strajhar P, Lavery GG, Schuster D, and Odermatt A (2013) Formation of threohydrobupropion from bupropion is dependent on 11β-hydroxysteroid dehydrogenase 1. *Drug Metab Dispos* **41**: 1671–1678.

Palovaara S, Pelkonen O, Uusitalo J, Lundgren S, and Laine K (2003) Inhibition of cytochrome P450 2B6 activity by hormone replacement therapy and oral contraceptive as measured by bupropion hydroxylation. *Clin Pharmacol Ther* **74**: 326–333.

Parkinson A, Kazmi F, Buckley DB, Yerino P, Ogilvie BW, and Paris BL (2010) System-dependent outcomes during the evaluation of drug candidates as inhibitors of cytochrome P450 (CYP) and uridine diphosphate glucuronosyltransferase (UGT) enzymes: human hepatocytes versus liver microsomes versus recombinant enzymes. *Drug Metab Pharmacokinet* **25**:16–27.

Petsalo A, Turpeinen M, and Tolonen A (2007) Identification of bupropion urinary metabolites by liquid chromatography/mass spectrometry. *Rapid Commun Mass Spectrom* **21**:2547–2554.

Posner J, Bye A, Dean K, Peck AW, and Whiteman PD (1985) The disposition of bupropion and its metabolites in healthy male volunteers after single and multiple doses. *Eur J Clin Pharmacol* **29**:97–103.

Reese MJ, Wurm RM, Muir KT, Generaux GT, St John-Williams L, and McConn DJ (2008) An in vitro mechanistic study to elucidate the desipramine/bupropion clinical drug-drug interaction. *Drug Metab Dispos* **36**:1198–1201.

Schroeder DH (1983) Metabolism and kinetics of bupropion. *J Clin Psychiatry* **44**: 79–81.

Silverstone PH, Williams R, McMahon L, Fleming R, and Fogarty S (2008) Convulsive liability of bupropion hydrochloride metabolites in Swiss albino mice. *Ann Gen Psychiatry* **7**:19.

Soroko FE, Mehta NB, Maxwell RA, Ferris RM, and Schroeder DH (1977) Bupropion hydrochloride ((+/-) alpha-t-butylamino-3-chloropropiophenone HCl): a novel antidepressant agent. *J Pharm Pharmacol* **29**:767–770.

Suckow RF, Smith TM, Perumal AS, and Cooper TB (1986) Pharmacokinetics of bupropion and metabolites in plasma and brain of rats, mice, and guinea pigs. *Drug Metab Dispos* **14**:692–697.

Suckow RF, Zhang MF, and Cooper TB (1997) Enantiomeric determination of the phenylmorpholinol metabolite of bupropion in human plasma using coupled achiral-chiral liquid chromatography. *Biomed Chromatogr* **11**:174–179.

Thase ME, Haight BR, Richard N, Rockett CB, Mitton M, Modell JG, VanMeter S, Harriett AE, and Wang Y (2005) Remission rates following antidepressant therapy with bupropion or selective serotonin reuptake inhibitors: a meta-analysis of original data from 7 randomized controlled trials. *J Clin Psychiatry* **66**:974–981.

Turpeinen M, Tolonen A, Uusitalo J, Jalonen J, Pelkonen O, and Laine K (2005) Effect of clopidogrel and ticlopidine on cytochrome P450 2B6 activity as measured by bupropion hydroxylation. *Clin Pharmacol Ther* **77**:553–559.

Welch RM, Lai AA, and Schroeder DH (1987) Pharmacological significance of the species differences in bupropion metabolism. *Xenobiotica* **17**:287–298.

Xu H, Loboz KK, Gross AS, and McLachlan AJ (2007) Stereoselective analysis of hydroxybupropion and application to drug interaction studies. *Chirality* **19**: 163–170.

Yanovski SZ and Yanovski JA (2015) Naltrexone extended-release plus bupropion extended-release for treatment of obesity. *JAMA* **313**:1213–1214.

Yee DA, Atayee RS, Best BM, and Ma JD (2014) Observations on the urine metabolic profile of codeine in pain patients. *J Anal Toxicol* **38**:86–91.

Yeung CK, Fujioka Y, Hachad H, Levy RH, and Isoherranen N (2011) Are circulating metabolites important in drug-drug interactions?: quantitative analysis of risk prediction and inhibitory potency. *Clin Pharmacol Ther* **89**:105–113.

Zhu AZ, Cox LS, Nollen N, Faseru B, Okuyemi KS, Ahluwalia JS, Benowitz NL, and Tyndale RF (2012) CYP2B6 and bupropion's smoking-cessation pharmacology: the role of hydroxybupropion. *Clin Pharmacol Ther* **92**:771–777.

Address correspondence to: Dr. Zeruesenay Desta, Division of Clinical Pharmacology, Department of Medicine, Indiana University School of Medicine, 950 W. Walnut Street, R2, Room 425, Indianapolis, IN 46202-5188. E-mail: zdesta@iu.edu